JOC The Journal of Organic Chemistry

Article

pubs.acs.org/joc

Monomer Emission and Aggregate Emission of an Imidazolium Macrocycle Based on Bridged Tetraphenylethylene and Their Quenching by C_{60}

Jin-Hua Wang,[†] Hai-Tao Feng,[†] Jun Luo,[‡] and Yan-Song Zheng*[,†]

[†]Key Laboratory for Large-Format Battery Materials and System, Ministry of Education, School of Chemistry and Chemical Engineering, Huazhong University of Science and Technology, Wuhan 430074, China

[‡]Tongji School of Pharmacy, Huazhong University of Science and Technology, Wuhan 430030, China

Supporting Information

ABSTRACT: A novel imidazolium macrocycle based on bridged tetraphenylethylene (TPE) was synthesized. Because it bears the bridged TPE units, this macrocycle not only displays an aggregation-induced emission (AIE) effect but also exhibits monomer emission, which is very rare in AIE compounds. With aggregation of the macrocycle, the aggregate emission increases while the monomer emission decreases. It was found that this imidazolium macrocycle can form a stable 2:1 complex with C_{60}, which gives rise to quenching of both the aggregate emission and the monomer emission. Unexpectedly, the aggregate emission exhibited a higher quenching efficiency than the monomer emission, probably because one adsorbed C_{60} molecule could affect more macrocycle molecules in the aggregate.

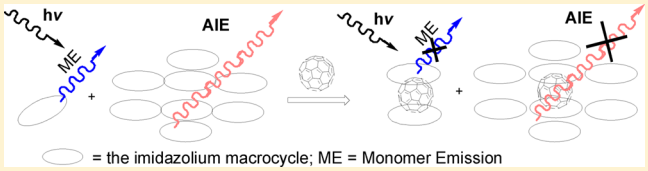

INTRODUCTION

In recent years, a new class of organic compounds that exhibit aggregation-induced emission (AIE) are attracting extensive attention because of their tremendous potential for use in chemosensors, bioprobes, and solid-state emitters.[1] These organic compounds emit no light in solution because of rotation of their substituents but exhibit fluorescence in the aggregated state. Upon partial fixation of the rotatable substituents, the AIE compounds probably also emit light in solution while they still keep the AIE effect. For example, tetraphenylethylene (TPE) is a typical AIE compound with no emission in solution. After two of its phenyl groups are connected by a single bond, the resulting bridged TPE exhibits emission even in solution as a result of restriction of the rotation of these two phenyl rings, which is ascribed to the emission of the bridged TPE monomer. In addition, the bridged TPE also emits fluorescence in the solid state because the retained two free phenyl rings can inhibit the $\pi-\pi$ stacking of the bridged TPE molecules.[2] If the monomer emission and the aggregation-induced emission appear simultaneously in the same medium, such as in a suspension, a dual-emission system can be obtained, which would allow the development of a new application area of AIE compounds in ratiometric sensing,[3] biomolecule tracking in living cells,[4] color tuning of solid-state emitters,[5] and so on. However, the bridged TPE is not reported to have monomer emission and AIE at the same time,[2] although a few other organic compounds can exhibit this property.[6] Here we report for the first time the synthesis of a novel imidazolium macrocycle based on bridged TPE. This macrocycle displays both AIE and monomer emission. Moreover, with aggregation of the macrocycle, the AIE increases while the monomer emission decreases, and both types of emission can be quenched by C_{60}.

RESULTS AND DISCUSSION

The imidazolium macrocycle **8** was synthesized using 9-fluorenone (**1**) and 4,4′-dimethoxybenzophenone (**2**) as starting materials (Scheme 1). They underwent a McMurry coupling reaction to give a 33% yield of TPE derivative **3** bearing two phenyl rings bridged by a valence bond. After **3** was transformed into the dialdehyde **4** by Duff reaction and then reduced to the dialcohol **5**, the bridged TPE dichloride **6** was obtained by treatment of **5** with thionyl chloride. Dichloride **6** was easily reacted with imidazole to give TPE diimidazole **7** in 91% yield via nucleophilic attack by imidazole. Finally, diimidazole **7** was further reacted with dichloride **6** in the presence of tetrabutylammonium chloride (TBACl) to provide imidazolium macrocycle **8** in 76% yield according to the reported procedure[7] with a little improvement. However, in the absence of the TBACl template, imidazolium macrocycle **8** was also obtained in almost the same yield. Therefore, the high yield of the imidazolium macrocycle was probably due to its poor solubility in the reaction solvent, which could drive the reaction to completion as the product precipitated.

As a salt, imidazolium macrocycle **8** displayed insolubility in less-polar organic solvents such as hexane and toluene, but it could easily be dissolved in DMSO and even exhibited some

Received: April 22, 2014
Published: May 28, 2014

dx.doi.org/10.1021/jo500884z | J. Org. Chem. 2014, 79, 5746−5751

Scheme 1. Synthesis of Imidazolium Macrocycle 8 Based on Bridged TPE

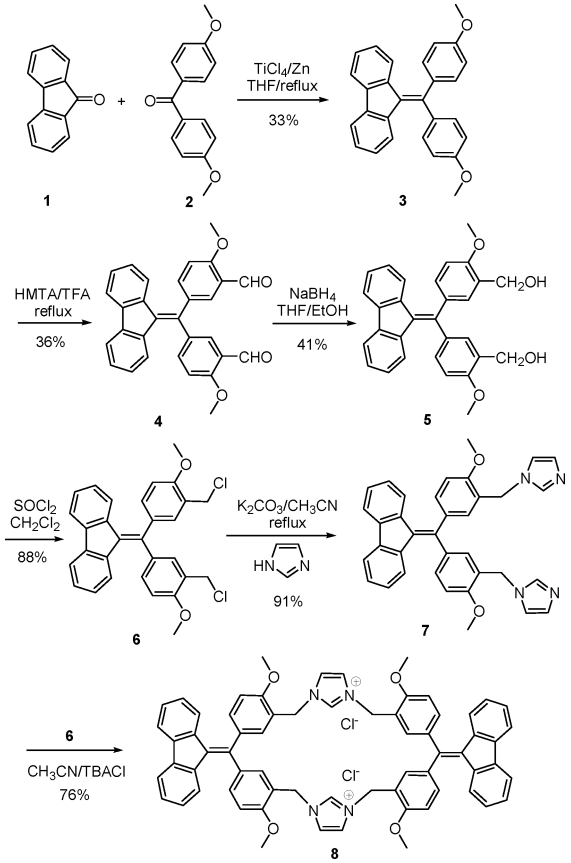

solubility in water and ethanol. Interestingly, a very dilute solution of **8** (1.0×10^{-5} M) in DMSO emitted fluorescence at 450 nm (Figure 1). With addition of the poor solvent toluene,

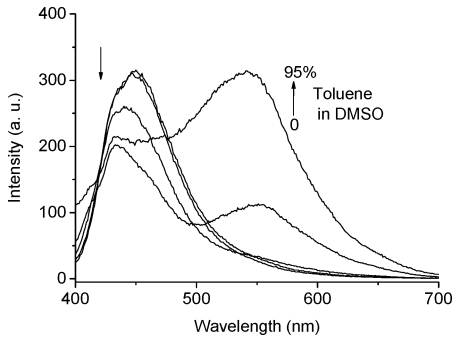

Figure 1. Changes in the fluorescence spectrum of **8** in DMSO upon addition of toluene. [**8**] = 1.0×10^{-5} M; toluene concentrations = 0, 20, 70, 90, and 95 vol %; λ_{ex} = 378 nm; ex/em slit widths = 5/10 nm.

not only did this emission decrease, but also its wavelength of maximum emission (λ_{max}^{em}) had a hypsochromic shift from 450 to 435 nm. Meanwhile, a new emission at 550 nm appeared when toluene was added until the solution became turbid. After that, the new emission rapidly increased with the continued addition of toluene. These results indicated that the emission at 450 nm should be ascribed to the monomer of **8** while the emission at 550 nm resulted from the aggregation of **8**. With addition of toluene, the increased aggregation would lead to a decrease in the monomer concentration of **8**, and therefore, the aggregate emission at 550 nm increased while the monomer emission at 450 nm decreased. At 95% toluene (all percentages or ratios related to solvents in this paper are of volume), the monomer emission should have been weaker than the monomer emission at 90% toluene, but the very strong aggregate emission at 550 nm raised the monomer emission to be stronger than that at 90% toluene.

To account for the effect of the solvent viscosity on the monomer emission, a solvent with lower viscosity (chloroform containing 2% DMSO to make the dissolution of **8** in chloroform easy) and a poor solvent (hexane with lower polarity) were used. The dilute solution of **8** in the mixed solvent of chloroform and DMSO (1.0×10^{-5} M) had a strong fluorescence at 440 nm. With the addition of hexane, this emission gradually decreased and λ_{max}^{em} exhibited a hypsochromic shift from 440 to 430 nm. When the hexane fraction was increased to 30%, the solution became turbid and a new emission at 555 nm appeared, and the emission at 440 nm decreased rapidly after this mixed ratio of the solvents (Figure 2). In addition, probably because of the lower polarity and lower viscosity of the solvent, the vibrational fine structure of the emission with three peaks at short wavelength could be made out. This further confirmed that this emission should be ascribed to the monomer. Similar to the results with the mixed solvent of DMSO and toluene, the monomer emission and the aggregate emission could simultaneously appear as long as the aggregation of the imidazolium macrocycle occurred. The fluorescence intensity change with changing solvent ratio also led to an obvious fluorescence color change of **8** from blue to red-orange to yellow-orange under irradiation at 365 nm using a UV lamp (Figure 2C). Interestingly, in the range of 20% to 60% hexane, the solution of **8** displayed a white-light emission property to a certain degree due to the combination of the blue color at the short wavelength and the yellow one at the long wavelength.

The viscosity of the solvent truly had a significant effect on the fluorescence of **8**. As shown in Figure 3A, the monomer emission increased rapidly with the glycerol fraction in DMSO, probably as a result of restriction of the intramolecular rotation (RIR) of **8**. Meanwhile, an obvious shoulder peak at about 550 nm started to appear when the glycerol fraction was increased to 60%, and it became stronger with the continued increase of the glycerol fraction. This hinted that aggregation of **8** in a viscous solvent also occurred. The absorption spectra of **8** showed a bathochromic shift (about 8 nm) with the viscosity of the solvent, indicating that the RIR led to the planarization of the TPE units of the macrocycle (Figure 3B). This was also the reason why the monomer emission also had a bathochromic shift (about 15 nm), while its intensity rapidly increased with the viscosity of the solvent (Figure 3A). As a result of the existing strong intermolecular interaction in an aggregate and the smaller effect of the viscosity on the molecules inside an aggregate, λ_{max}^{em} for the aggregate emission (550 nm) showed no shift with the viscosity. In contrast, the suspension of **8** in 95:5 toluene/DMSO or 90:10 hexane/$CHCl_3$ had almost the same absorption maximum wavelength (387 nm) as the solution of **8** in the corresponding DMSO or $CHCl_3$, but the absorbance was attenuated as a result of the aggregation (Figures S9–S11 in the Supporting Information).

Because of the solubility of **8** in water, the changes in the monomer emission and the aggregation in aqueous media as the solvent ratio was varied were studied. In the 95:5 water/DMSO mixed solvent, the aggregate emission was major while

dx.doi.org/10.1021/jo500884z | J. Org. Chem. 2014, 79, 5746–5751

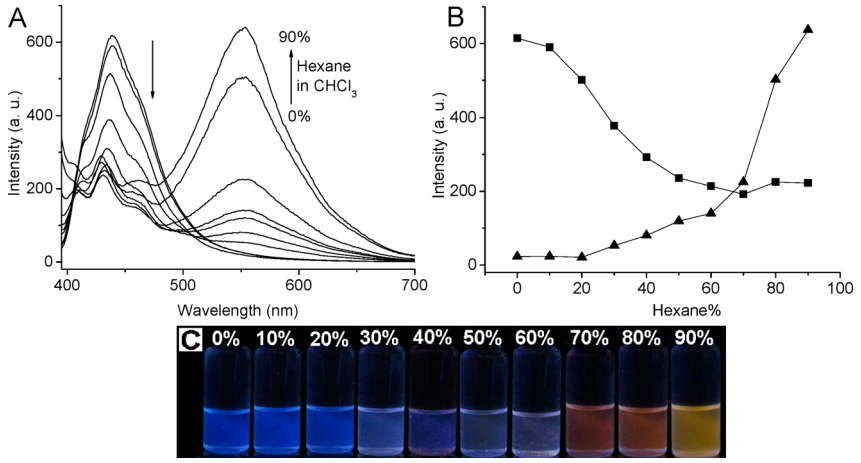

Figure 2. (A) Changes in the fluorescence spectrum of **8** with hexane fraction in $CHCl_3$ containing 2% DMSO. (B) Plots of the fluorescence intensities of **8** at 442 nm (■) and 554 nm (▲) vs hexane fraction. (C) Photos of **8** in $CHCl_3$ containing 2% DMSO with different hexane fractions under 365 nm lamp light. [**8**] = 1.0×10^{-5} M; λ_{ex} = 378 nm; ex/em slit widths = 5/10 nm.

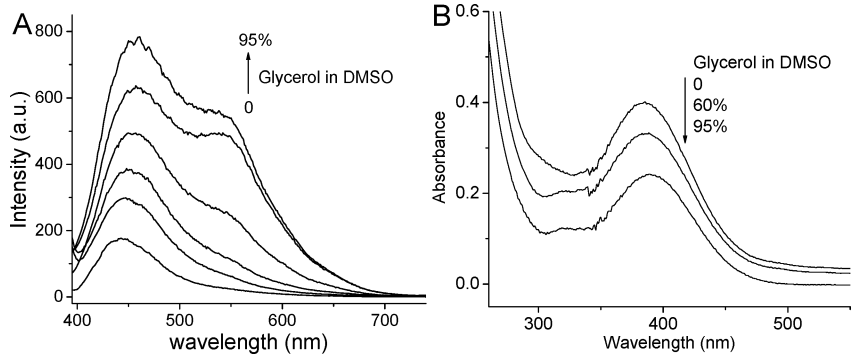

Figure 3. (A) Changes in the fluorescence spectrum of **8** in DMSO as the glycerol fraction was varied from 0 to 20, 40, 60, 80, and 95%. (B) Changes in the UV−vis spectrum of **8** in DMSO as the glycerol fraction was varied from 0 to 60 and 95%. [**8**] = 1.0×10^{-5} M; λ_{ex} = 378 nm; ex/em slit widths = 5/10 nm.

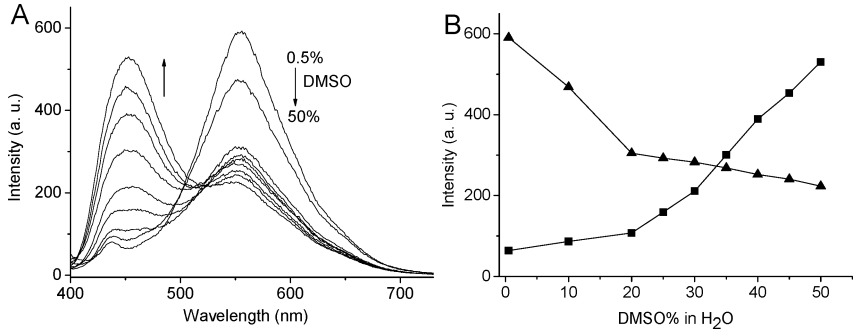

Figure 4. (A) Changes in the fluorescence spectrum of **8** with DMSO fraction in H_2O. (B) Plots of the fluorescence intensities of **8** at 442 nm (■) and 554 nm (▲) vs DMSO fraction. [**8**] = 2.5×10^{-5} M; λ_{ex} = 378 nm; ex/em slit widths = 10/10 nm.

the monomer emission was minor because the molecules of **8**, just like amphiphilic compounds, mainly existed in the aggregated state in water. As the DMSO fraction was increased, the aggregate emission gradually decreased while the monomer emission increased because of the good solubility of **8** in DMSO (Figure 4). These results indicated that the intensity of the monomer emission and the aggregation could be adjusted by changing the solvent ratio in aqueous media, which would be beneficial for using **8** to detect some biological compounds in water.

As the concentration of **8** in DMSO was increased from 1.0×10^{-5} to 1.0×10^{-3} M, the monomer emission at 450 nm gradually decreased but the emission at about 550 nm did not increase, which displayed the same phenomenon as the general fluorescence molecules. However, when the concentration was increased to 1.0×10^{-3} M, the emission at about 550 nm started to appear while the monomer fluorescence at 450 nm was completely quenched (Figure 5). These results indicated that the emission at the longer wavelength should not be ascribed to an excimer of the macrocycle **8** but instead resulted

dx.doi.org/10.1021/jo500884z | J. Org. Chem. 2014, 79, 5746−5751

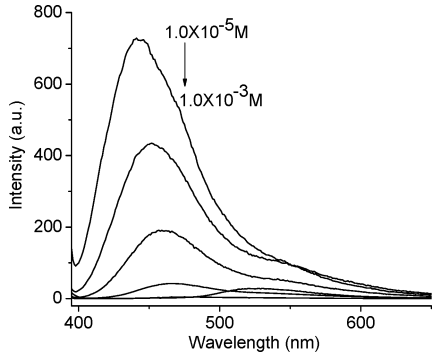

Figure 5. Changes in the fluorescence spectrum of **8** in DMSO as the concentration of **8** increased from 1.0 to 2.5, 5.0, 10.0, 20.0, and 100 × 10^{-5} M. λ_{ex} = 378 nm; ex/em slit widths = 10/10 nm.

from the aggregation because the macrocycle **8** at a very large concentration probably started to aggregate.

The excitation spectra of **8** monitored at the shorter emission wavelength (453 nm) and the longer emission wavelength (555 nm) were measured (Figure 6). One excitation spectrum had

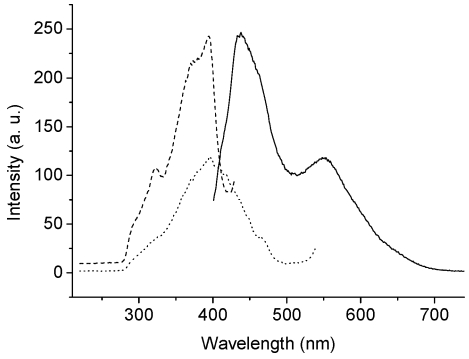

Figure 6. Excitation spectra of **8** monitored at 443 nm (dashed line) and 555 nm (dotted line) and its emission spectrum (solid line) in 1:9 DMSO/toluene. [**8**] = 1.0 × 10^{-5} M; λ_{ex} = 378 nm for the emission spectrum; ex/em slit widths = 5/10 nm.

an excitation maximum wavelength of 396 nm while the other one had the excitation maximum at 400 nm, and the two spectra had different band shapes, demonstrating that the monomer emission and the aggregate emission resulted from different chemical species.

It has been reported that macrocycles composed of imidazolium units can bind fullerene C_{60} by cation−π interactions,[8a] besides associating with a wide variety of anions by electrostatic interactions.[8] The cation−π interactions probably lead to fluorescence quenching of **8**, and therefore, C_{60} was initially used to test the sensing property of **8** for analytes. In 1:1 DMSO/toluene as the solvent, **8** exhibited only the monomer emission at 460 nm. With the addition of C_{60}, the fluorescence intensity gradually decreased. After 3 equiv of C_{60} was added, the monomer fluorescence was basically quenched (Figure 7). From the exponential quenching equation $I_0/I = Ae^{k[Q]} + B$,[9] the quenching constant for the monomer emission of **8** by C_{60} was calculated to be $k = 1.28 \times 10^4$ M^{-1} (Figure S12 in the Supporting Information); this large value demonstrates a strong interaction between **8** and C_{60}. From the Job's plot for the fluorescence titration, the **8**:C_{60} binding ratio was 2:1 (Figure S13 in the Supporting Information),

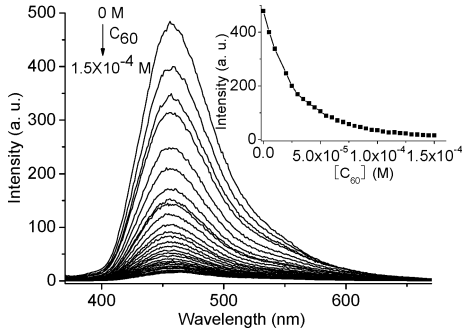

Figure 7. Change in the fluorescence spectrum of **8** with C_{60} concentration in 1:1 DMSO/toluene. The inset shows a plot of the fluorescence intensity at 460 nm vs the concentration of C_{60}. [**8**] = 5.0 × 10^{-5} M; [C_{60}] = 0 to 1.5 × 10^{-4} M; λ_{ex} = 350 nm; ex/em slit widths = 5/10 nm.

indicating that **8** and C_{60} probably form a complex having a sandwich structure.

In the 1:9 DMSO/toluene solvent where **8** exhibited dual emission, the fluorescence intensity change with C_{60} concentration was also measured (Figure 8). As C_{60} was gradually added, both the monomer emission at the shorter wavelength (453 nm) and the aggregate emission at the longer wavelength (555 nm) decreased. However, the aggregate fluorescence was quenched more rapidly than the monomer one. The change in the fluorescence intensity ratio (I_0/I) for **8** without and with C_{60} at 555 nm versus the concentration of C_{60} was obviously exponential. The change at 453 nm was also exponential if the curve was magnified (Figure S14 in the Supporting Information). The quenching constants for the aggregate fluorescence and the monomer fluorescence were 3.3 × 10^4 and 2.6 × 10^4 M^{-1}, respectively (Figure S14).

It would be expected that C_{60} molecules would need to diffuse into the inside of an aggregate before they could contact all of the molecules of **8** in the aggregate. On the other hand, C_{60} molecules could easily contact the monomers of **8** in solution without the need to diffuse. Therefore, the monomer fluorescence should be quenched more efficiently than the aggregate fluorescence by C_{60}. However, the result was contrary to this inference. It is probable that there is an interaction among multiple molecules of **8** in an aggregate that is pivotal to the aggregate emission. If this interaction is interrupted by one C_{60} molecule, the fluorescence from the multiple molecules in the aggregate of **8** could be quenched. Unlike the quenching of the monomer emission, it would not be necessary to quench every molecule in the aggregate by C_{60} molecules. Therefore, the quenching of the aggregate fluorescence is more efficient than that of the monomer fluorescence. This is in accordance with some literature reports in which the fluorescence of a solid is much more easily quenched than that of a solution.[10]

To further disclose the interaction of **8** with C_{60}, a UV−vis titration of C_{60} with **8** was carried out. As shown in Figure 9, the absorbance of C_{60} at wavelengths longer than 509 nm decreased while the absorbance at wavelengths shorter than 509 nm increased with addition of **8**. There was a clear isosbestic point at 509 nm. In addition, an obvious color change from red-purple to yellow could be observed during the titration. This demonstrates that a stable complex of **8** with C_{60} was produced. From the Job's plot (Figure S15 in the Supporting Information), the complex of **8** with C_{60} had an **8**:C_{60} binding ratio of 2:1, in accordance with the result from the fluorescence

dx.doi.org/10.1021/jo500884z | J. Org. Chem. 2014, 79, 5746−5751

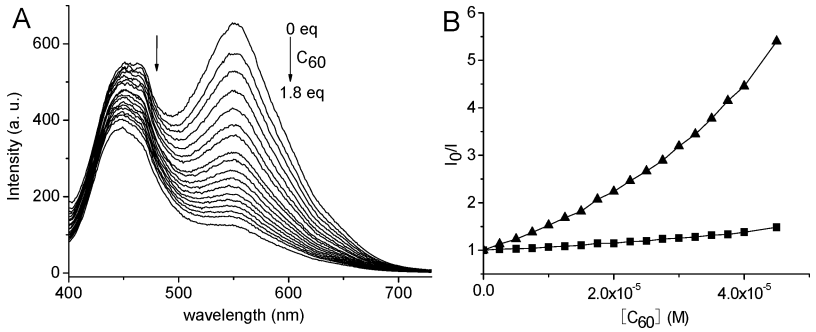

Figure 8. (A) Changes in the dual-emission spectrum of **8** with the amount of C_{60} in 1:9 DMSO/toluene. (B) Plots of the fluorescence intensity ratios I_0/I (without C_{60}/with C_{60}) of **8** at 453 nm (■) and 555 nm (▲) vs C_{60} concentration. [**8**] = 2.5 × 10^{-5} M; λ_{ex} = 378 nm; ex/em slit widths = 5/10 nm.

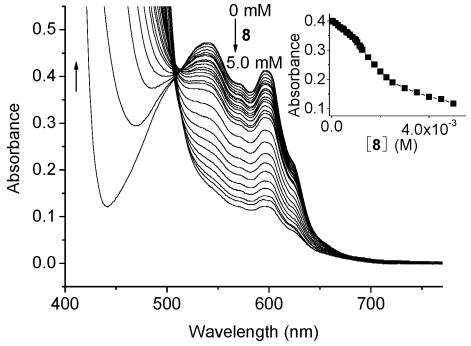

Figure 9. Changes in the UV−vis spectrum of C_{60} in 1:1 DMSO/toluene with the addition of **8**. The inset shows a plot of the absorbance of C_{60} at 600 nm vs the concentration of **8**. [C_{60}] = 5.0 × 10^{-4} M.

titration. The association constant of the $\mathbf{8}_2$·C_{60} complex was calculated to be (5.26 ± 0.29) × 10^5 M^{-2} by nonlinear curve fitting of the absorbance at 600 nm versus the concentration of **8** (Figure S16 in the Supporting Information).[11]

■ CONCLUSION

A novel imidazolium macrocycle containing bridged tetraphenylethylene (TPE) was synthesized. Because it bears the bridged TPE units, this macrocycle not only displays an AIE effect but also exhibits monomer emission, which is very rare in organic compounds having an AIE effect. With aggregation of the macrocycle, the aggregate emission increased while the monomer emission decreased. Because of cation−π interactions, this imidazolium macrocycle can form a stable 2:1 complex with C_{60}, which results in quenching of both the aggregation emission and the monomer emission. Moreover, the aggregate emission exhibits a higher quenching efficiency than the monomer emission, probably because one adsorbed C_{60} molecule breaks the interaction among multiple molecules in the aggregate that is pivotal to the aggregate emission. This dual-emission phenomenon will endow AIE compounds with greater application potential.

■ EXPERIMENTAL SECTION

Materials and Methods. Reagents and solvents were chemically pure (CP) grade or analytical reagent (AR) grade and were used as received, unless otherwise specified. ^{1}H and ^{13}C NMR spectra were measured on a 400 MHz NMR spectrometer at 298 K in DMSO-d_6. Infrared spectra were recorded on an IR spectrometer. Absorption spectra were recorded on a UV−vis spectrophotometer. Mass spectra were measured on an FTMS instrument. Fluorescent emission spectra were collected on a fluorophotometer at 298 K.

Preparation of Bridged TPE Derivative 3. The preparation was carried out according to the literature.[12] A flask equipped with a magnetic stirrer was charged with zinc dust (16 g, 160 mmol) and THF (100 mL) under a nitrogen atmosphere. The mixture was cooled to 0 °C, and $TiCl_4$ (8.8 mL, 80 mmol) was added slowly by syringe. After the mixture was heated to reflux for 2.5 h, it was cooled to ambient temperature. Then 4,4′-dimethoxybenzophenone (**2**) and 9-fluorenone (**1**) (1:1.5 molar ratio, total of 10 mmol) in THF (60 mL) were added, and the mixture was refluxed for 12 h. The reaction was quenched with 10% K_2CO_3 aqueous solution (100 mL), and the resulting mixture was extracted with dichloromethane. The organic layer was desiccated with anhydrous sodium sulfate, filtered, and evaporated to dryness under vacuum. The residue was purified by column chromatography to give a yellow powder (1.3 g, 33%).

Preparation of Dialdehyde 4. A flask was charged with **3** (1.0 g, 2.56 mmol), hexamethylenetetramine (3.58 g, 25.6 mmol), and trifluoroacetic acid (20 mL). The resultant mixture was refluxed under stirring for 30 min and then cooled to room temperature. The reaction was quenched with 15 mL of water, and the mixture was stirred for 4 h and then extracted with dichloromethane (3 × 25 mL). The combined organic layers were desiccated with anhydrous sodium sulfate, filtered, and evaporated to dryness under vacuum. The resultant slurry was purified with column chromatography to give a orange-red powder (410 mg, 36%). The resultant slurry was purified by column chromatography to give an orange-red powder (410 mg, 36%) as a mixture of **4** and another minor multialdehyde compound that was hard to be separated from **4**. The mixture was directly used in the next reaction without further purification.

Preparation of Dialcohol 5. A flask was charged with **4** (410 mg, 0.92 mmol), $NaBH_4$ (350 mg, 9.19 mmol), and EtOH/THF (3:2 v/v, 25 mL total). The mixture was stirred at ambient temperature for 3 h, washed with water, and extracted with dichloromethane (3 × 25 mL). The combined organic layers were desiccated with anhydrous sodium sulfate, filtered, and evaporated to dryness under vacuum. The residue was subjected to column chromatography to give a yellow powder (170 mg, 41%). Mp 258−260 °C; ^{1}H NMR (400 MHz, $CDCl_3$) δ (ppm) 7.74 (s, 2H), 7.26 (d, J = 6.1 Hz, 2H), 7.25 (s, 2H), 7.1−6.9 (m, 6H), 6.78 (d, J = 8.1 Hz, 2H), 4.72 (s, 4H), 3.88 (s, 6H); ^{13}C NMR (100 MHz, $CDCl_3$) δ (ppm) 160.0, 145.8, 140.3, 140.0, 139.1, 135.4, 132.6, 132.0, 125.2, 124.6, 117.8, 114.0, 65.5, 55.3; IR (KBr) ν 3430, 3029, 2954, 2928, 2869, 2838, 1627, 1604, 1573, 1507, 1461, 1412, 1362, 1330, 1286, 1248, 1179, 1153, 1109, 1086, 1033, 919, 884, 858, 834, 784, 762, 732, 664, 621, 596, 544, 422 cm^{-1}; ESI^+ HRMS m/z calcd for $C_{30}H_{26}O_4$ 450.1831 [M^+], found 450.1837.

Preparation of Dichloride 6. A flask was charged with **5** (180 mg, 0.4 mmol), pyridine (60 μL, 0.8 mmol), and dichloromethane (10 mL). After the mixture was stirred at room temperature for 10 min, a solution of $SOCl_2$ (0.17 mL) in dichloromethane (5 mL) was added dropwise over 30 min. The mixture was heated at 40 °C under stirring for 6 h and then quenched and washed with water. The combined

dx.doi.org/10.1021/jo500884z | J. Org. Chem. 2014, 79, 5746−5751

organic phases were desiccated with anhydrous sodium sulfate, filtered, and evaporated to dryness under vacuum. The residue was recrystallized with CH_2Cl_2 and MeOH to give a yellow solid (172 mg, 88%). Mp 193−195 °C; ^{1}H NMR (400 MHz, $CDCl_3$) δ (ppm) 7.75 (d, J = 1.2 Hz, 2H), 7.25 (d, J = 5.8 Hz, 4H), 6.97−6.89 (m, 2H), 6.92 (d, J = 8.7 Hz, 4H), 6.78 (d, J = 8.2 Hz, 2H), 4.63 (s, 4H), 3.88 (s, 6H); ^{13}C NMR (100 MHz, $CDCl_3$) δ (ppm) 160.2, 147.2, 140.0, 139.7, 136.3, 135.1, 132.2, 132.1, 126.9, 124.7, 119.5, 114.0, 55.4, 46.6; IR (KBr) ν 2930, 1601, 1571, 1505, 1455, 1413, 1335, 1296, 1250, 1174, 1110, 1032, 909, 834, 811, 730, 693, 635, 598, 543 cm^{-1}; ESI$^+$ HRMS m/z calcd for $C_{30}H_{24}Cl_2O_2$ 486.1153 [M$^+$], found 486.1133.

Synthesis of Diimidazole 7. To a flask were added **6** (96 mg, 0.2 mmol), imidazole (136 mg, 2 mmol), potassium carbonate (54 mg, 0.4 mmol), and redistilled CH_3CN (8 mL). After the mixture was refluxed under stirring for 5 h, it was cooled to room temperature, washed with water, and extracted with dichloromethane (3 × 15 mL). The combined organic layers were desiccated with anhydrous sodium sulfate, filtered, and evaporated to dryness under vacuum. The residue was purified by column chromatography to give a yellow powder (100 mg, 91%). Mp 204.3−205.7 °C; ^{1}H NMR (400 MHz, $CDCl_3$) δ (ppm) 7.58 (s, 2H), 7.45 (s, 2H), 7.23 (d, J = 8.6 Hz, 4H), 7.09 (s, 2H), 6.92 (s, 2H), 6.91 (d, J = 8.6 Hz, 4H), 6.78 (s, 4H), 5.13 (s, 4H), 3.87 (s, 6H); ^{13}C NMR (100 MHz, CDCl3) δ (ppm) 160.2, 147.4, 140.0, 139.5, 137.4, 135.0, 132.0, 131.9, 129.8, 125.8, 125.0, 119.3, 118.2, 114.1, 55.3, 50.9; FTIR (KBr) ν 3439, 2929, 1601, 1571, 1506, 1443, 1416, 1389, 1291, 1248, 1175, 1108, 1075, 1028, 906, 820, 737, 663, 630, 598 cm^{-1}; ESI$^+$ HRMS m/z calcd for $C_{36}H_{31}N_4O_2$ 551.2447 [M + H]$^+$, found 551.2422.

Synthesis of Imidazolium Macrocycle 8. To a flask were added **6** (106 mg, 0.19 mmol), **7** (94 mg, 0.19 mmol), TBACl (268 mg, 0.96 mmol), and acetonitrile (8 mL). After the mixture was refluxed for 12 h under stirring and then cooled to room temperature, the resultant precipitate was collected by filtration and washed with dichloromethane to give a red-yellow powder (150 mg, 76%). Mp 251.4−253.2 °C; ^{1}H NMR (400 MHz, DMSO-d_6) δ 9.36 (s, 2H), 7.59 (s, 4H), 7.81 (s, 4H), 7.24 (d, J = 8.0 Hz, 4H), 7.20 (d, J = 8.4 Hz, 8H), 7.04 (d, J = 8.8 Hz, 8H), 6.67 (d, J = 8.4 Hz, 4H), 5.41 (s, 8H), 3.84 (s, 12H); ^{13}C NMR (100 MHz, DMSO-d_6) δ 159.8, 147.9, 139.6, 139.4, 139.1, 138.9, 135.7, 134.3, 133.2, 131.2, 131.0, 127.9, 123.9, 122.7, 120.7, 114.3, 55.2, 52.1; IR (KBr) ν 3398, 3135, 3055, 3004, 2958, 2835, 1595, 1563, 1501, 1447, 1412, 1358, 1290, 1244, 1170, 1142, 1107, 1021, 966, 897, 819, 776, 732, 586, 537, 472 cm^{-1}; ESI$^+$ HRMS m/z calcd for $C_{66}H_{54}ClN_4O_4$ 1001.3833 [M − Cl]$^+$, found 1001.3835.

■ ASSOCIATED CONTENT

Ⓢ Supporting Information

Experimental details, spectra of compounds, and calculation of association constants. This material is available free of charge via the Internet at http://pubs.acs.org.

■ AUTHOR INFORMATION

Corresponding Author

*E-mail: zyansong@hotmail.com.

Notes

The authors declare no competing financial interest.

■ ACKNOWLEDGMENTS

This research work was supported by the National Natural Science Foundation of China (21072067) and the Analytical and Testing Centre at Huazhong University of Science and Technology.

■ REFERENCES

(1) Reviews of AIE compounds: (a) Hong, Y.; Lam, J. W. Y.; Tang, B. Z. *Chem. Soc. Rev.* **2011**, *40*, 5361−5388. (b) Hong, Y.; Lam, J. W. Y.; Tang, B. Z. *Chem. Commun.* **2009**, 4332−4353. (c) Ding, D.; Li, K.; Liu, B.; Tang, B. Z. *Acc. Chem. Res.* **2013**, *46*, 2441−2453. (d) Wang, M.; Zhang, G.; Zhang, D.; Zhu, D.; Tang, B. Z. *J. Mater. Chem.* **2010**, *20*, 1858−1867.

(2) (a) Shi, J.; Chang, N.; Li, C.; Mei, J.; Deng, C.; Luo, X.; Liu, Z.; Bo, Z.; Dong, Y. Q.; Tang, B. Z. *Chem. Commun.* **2012**, *48*, 10675−10677. (b) Tong, H.; Dong, Y.; Hong, Y.; Häussler, M.; Lam, J. W. Y.; Sung, H. H.-Y.; Yu, X.; Sun, J.; Williams, I. D.; Kwok, H. S.; Tang, B. Z. *J. Phys. Chem. C* **2007**, *111*, 2287−2294.

(3) (a) McLaurin, E. J.; Bradshaw, L. R.; Gamelin, D. R. *Chem. Mater.* **2013**, *25*, 1283−1292. (b) Zhang, K.; Zhou, H.; Mei, Q.; Wang, S.; Guan, G.; Liu, R.; Zhang, J.; Zhang, Z. *J. Am. Chem. Soc.* **2011**, *133*, 8424−8427. (c) Liu, X.; Zhang, N.; Bing, T.; Shangguan, D. *Anal. Chem.* **2014**, *86*, 2289−2296.

(4) (a) Zhang, G.; Palmer, G. M.; Dewhirst, M. W.; Fraser, C. L. *Nat. Mater.* **2009**, *8*, 747−751. (b) Chen, T.; Hu, Y.; Cen, Y.; Chu, X.; Lu, Y. *J. Am. Chem. Soc.* **2013**, *135*, 11595−11602. (c) Zhu, A.; Qu, Q.; Shao, X.; Kong, B.; Tian, Y. *Angew. Chem., Int. Ed.* **2012**, *51*, 7185−7189.

(5) (a) Liu, Y.; Pan, M.; Yang, Q.-Y.; Fu, L.; Li, K.; Wei, S.-C.; Su, C.-Y. *Chem. Mater.* **2012**, *24*, 1954−1960. (b) Gorris, H. H.; Ali, R.; Saleh, S. M.; Wolfbeis, O. S. *Adv. Mater.* **2011**, *23*, 1652−1655. (c) Chen, O.; Shelby, D. E.; Yang, Y.; Zhuang, J.; Wang, T.; Niu, C.; Omenetto, N.; Cao, Y. C. *Angew. Chem., Int. Ed.* **2010**, *49*, 10132−10135.

(6) (a) Kohmoto, S.; Tsuyuki, R.; Hara, Y.; Kaji, A.; Takahashi, M.; Kishikawa, K. *Chem. Commun.* **2011**, *47*, 9158−9160. (b) Neelakandan, P. P.; Ramaiah, D. *Angew. Chem., Int. Ed.* **2008**, *47*, 8407−8411. (c) Nandajan, P. C.; Neelakandan, P. P.; Ramaiah, D. *RSC Adv.* **2013**, *3*, 5624−5630.

(7) Alcalda, E.; Ramos, S.; Garcia, L. P. *Org. Lett.* **1999**, *1*, 1035−1038.

(8) (a) Chun, Y.; Singh, N. J.; Hwang, I.-C.; Lee, J. W.; Yu, S. U.; Kim, K. S. *Nat. Commun.* **2013**, *4*, No. 1797. (b) Zhou, H.; Zhao, Y.; Gao, G.; Li, S.; Lan, J.; You, J. *J. Am. Chem. Soc.* **2013**, *135*, 14908−14911. (c) Shirinfar, B.; Ahmed, N.; Park, Y. S.; Cho, G.-S.; Youn, S.; Han, J.-K.; Nam, H. G.; Kim, K. S. *J. Am. Chem. Soc.* **2013**, *135*, 90−93.

(9) Liu, J.-Z.; Zhong, Y.-C.; Lu, P.; Hong, Y.-N.; Lam, J. W. Y.; Faisal, M.; Yu, Y.; Wong, K. S.; Tang, B.-Z. *Polym. Chem.* **2010**, *1*, 426−429.

(10) (a) Kartha, K. K.; Babu, S. S.; Srinivasan, S.; Ajayaghosh, A. *J. Am. Chem. Soc.* **2012**, *134*, 4834−4841. (b) Tan, C.; Atas, E.; Müller, J. G.; Pinto, M. R.; Kleiman, V. D.; Schanze, K. S. *J. Am. Chem. Soc.* **2004**, *126*, 13685−13694.

(11) Feng, H.-T.; Song, S.; Chen, Y.-C.; Shen, C.-H.; Zheng, Y.-S. *J. Mater. Chem. C* **2014**, *2*, 2353−2359.

(12) Luo, X.; Li, J.; Li, C.; Heng, L.; Dong, Y. Q.; Liu, Z.; Bo, Z.; Tang, B. Z. *Adv. Mater.* **2011**, *23*, 3261−3265.